Available online at www.sciencedirect.com
SCIENCE DIRECT®
Journal of Nuclear Materials 329–333 (2004) 513–517
journal of nuclear materials
www.elsevier.com/locate/jnucmat

The investigation of crack mechanism for Tyranno-SA SiC/SiC composites with ESI method

J.Y. Yan [a,*], C.W. Chen [a], P.C. Fang [a], K.M. Yin [a], F.R. Chen [a], Y. Katoh [b], A. Kohyama [b], J.J. Kai [a]

[a] *Department of Engineering and System Science, National Tsing-Hua University, 101, Section 2, Kuang-Fu Rd., Hsinchu 300, Taiwan, ROC*

[b] *Institute of Advanced Energy, Kyoto University, Gokasho, Uji, Kyoto 611-0011, Japan*

Abstract

In order to clarify the fracture mechanism of frictional stress and bonding strength in SiC/SiC composites, the mechanical test and HRTEM equipped with electron energy loss spectrometer were used. Due to the high sensitivity of carbon k-edge in the EELS spectrum, EELS is more convenient than other analytical tools. The advanced electronic spectroscopic image (ESI) technique is applied to observe the wide area around the interface of SiC fiber/pyrolytic carbon/SiC matrix. The sp^2 fraction mapping reveals the non-uniform and high sp^2 concentration existence at the interface of fiber/pyrolytic carbon. This result proves the cracking start at this region and extends to whole specimen.

1. Introduction

SiC fiber reinforced SiC matrix composites (SiC/SiC) are well-known materials with promise for high temperature applications such as fusion reactor, airplane... etc., because of superior chemical and mechanical stability at high temperature, low induced-activation energy and afterheat [1–3]. However, the intrinsic properties of SiC/SiC composites are predominated by fabrication processing. There are various conventional manufacturing techniques for SiC composites such as chemical vapor infiltration (CVI), polymer impregnation and pyrolysis (PIP) and hot pressing (HP) [4–6]. The goal of these processes is to take an advantage of the strong fiber and matrix (F/M) interface to resist radiation damage. The damage usually induces the debonding of the F/M interface and leads to crack penetration through the SiC/SiC composites. Therefore, it is well recognized that the quality of the F/M interface is a key role in determining the properties of the SiC/SiC composites [7]. In order to reinforce the quality of the interface, the behavior of the pyrolytic carbon (PyC) interphase must be investigated since it is the most efficient parameter [8,9]. Recently, the high stoichiometric SiC fiber, the PyC Tyranno-SA (Ube Industries, Ltd., Ube, Japan), fabricated with CVI process has been used in irradiation research because of several advantages like high purity, high crystallization of matrix and low oxidation for the carbon interphase [10].

However, to interpret the characteristic of F/M interface merely with SEM images with the mechanical tests is not enough because the SEM images are not possible to determine, the cracking in the PyC interphase is generated from matrix or fiber side precisely. To understand the characteristic of the carbon interphase, the mechanical test and microstructure analysis are necessary. In this article, the 2D woven PyC Tyranno SA SiC/SiC composite is used to study the PyC interphase with fiber pull-out tension test [7,10] and high resolution TEM equipped electron energy loss spectroscopy (EELS). The former analysis can extract the

* Corresponding author. Tel.: +886-3 5715131 4282; fax: +886-3 5734066.
E-mail address: d887101@oz.nthu.edu.tw (J.Y. Yan).

0022-3115/$ - see front matter © 2004 Published by Elsevier B.V.
doi:10.1016/j.jnucmat.2004.04.342

interfacial debonding strength and frictional stress information that all of the mechanical properties and the latter can provide the microstructure and bonding strength of F/M interface. The EELS is very powerful analytical tool for carbon materials properties because the concentration of π (sp^2) and σ (sp^3) bonding can be distinguished clearly [11] and the mechanical properties of carbon such as bonding strength, Young's modulus and hardness are proportional to the ratio of π and σ bonding [12–14]. The EFTEM combined with TEM and EELS can provide 2-D area information by mapping technique, which owns high spatial resolution and characteristic distribution.

2. Experimental

Two-dimensional woven Tyranno-SA/PyC/SiC_{CVI} composites were fabricated via chemical vapor infiltration (CVI) by Institute of Advanced Energy of Kyoto University. Prior to matrix infiltration, Propylene (C_3H_6) gas was used to deposit carbon interphase (50–150 nm) by chemical vapor deposition (CVD) at 1100 °C with a carrier gas of argon and this method results in a low-oxygen content in the carbon layer. The mechanical properties as fiber pull-out tension tests is using a load controlled micro-indentation testing system with triangular diamond pyramidal indenter. The pull-out fibers were examined by the field emission scanning microscopy (FE-SEM). The detailed procedure and results was described in the previous study [7]. The JEOL 2010F field emission TEM equipped with Gatan image filter (GIF) is employed to analyze the microstructure and bonding of SiC/SiC composite which is not treated with mechanical test. For EEL-spectra analysis, there are two main energy loss regions could be used. First is the low-loss region where the energy loss below 100 eV is also called plasmon energy region because the absorption was caused by the plasmon oscillation. In this region, the specific energy loss is caused by the plasma oscillation and could be described with Drude formula [15]

$$E_P = \hbar(Ne^2/m_e\varepsilon_0)^{1/2}, \quad (1)$$

where N is the valence electron density, $\hbar$ is the Planck constant, e is the electron charge, ε_0 is the permittivity of the free space and m_e is the electron effective mass. The other region is named core-loss region which is generated by energy loss from exciting the core electron to the unoccupied state. Comparing these regions, the advantages of low-loss region are high signal-to-noise (S/N) ratio and very short acquisition time. Unfortunately, the loss of spatial resolution in the low-loss region caused by delocalization and artifacts from the strong diffraction contrast [16,17] result in the low-loss region is not suitable for nanoscale analysis and mapping technique. Hence, the core-loss absorption is determined for analyzing the PyC interphase layer behavior.

In order to identify the origin of the cracking in the Tyranno-SA SiC/SiC composites, the two dimensional advanced electron spectroscopic imaging (ESI) method which developed from EEL-spectra analysis technique was used. The ESI method was first proposed by Jeanguillaume et al. [18] and other electron microscopists [11,19–23]. However, the traditional ESI method has some innate drawbacks such as poor energy resolution, blur energy distribution due to convolution effect, lower sampling in energy space and specimen drift. Although ESI technique provides nanoscale 2-D information, these drawbacks would reduce reliability. To overcome these problems, several numerical methods are embedded into the ESI technique and named advanced ESI method [22,23]. The model-free fast Fourier transformation, FFT, interpolation is used to increase the sampling in the energy space, the maximum entropy method (MEM) and Fourier ratio deconvolution method are used to eliminate the convolution effect from the energy slit and specimen thickness, and the wavelet transformation shrinkage is employed to reduce the artifacts and noise contribution. The detailed discussion of these methods can be found in our previous studies [23]. After these numerical processing, the advanced ESI spectra are almost matched with the EEL-spectra and beneficial for π and σ bonding quantification. According to the EELS Atlas, carbon k-edge absorption energy for π and σ bonding are located at the 283.5 and 292 eV. Therefore, the operation condition of ESI method sets as follows: the energy range is from 240 to 340 eV, the energy slit is 4 eV and acquired time is 6 s. Total specimen drift after acquired 26 energy loss images (160 s) is restricted about 1nm. The ESI-spectrum is extracted from 3×3 pixels and the spatial resolution of ESI image is 0.9 nm^2/unit. After processing with advanced ESI methods, the energy dispersion is increased from 4 to 0.125 eV/ch by model-free FFT interpolation because there is no suitable model for EELS core-loss spectra. The convolution effect of thickness and energy slit is removed by MEM and Fourier ratio method. The energy resolution is also improved from 4 to 0.87 eV.

3. Results and discussion

Fig. 1 is the set of SEM images for the Tyranno-SA SiC/SiC composites after the typical pull-out tests. The Fig. 1(a) shows the roughness surface morphology of the pull-out fiber. The high magnification image of the push-out fiber is shown in the Fig. 1(b). The clear interfacial morphology is represented and displays the non-uniform cracking surface of PyC interphase in the axial and vertical direction. The bright field TEM image of Tyranno-SA SiC/SiC composite is shown in the Fig. 2. In

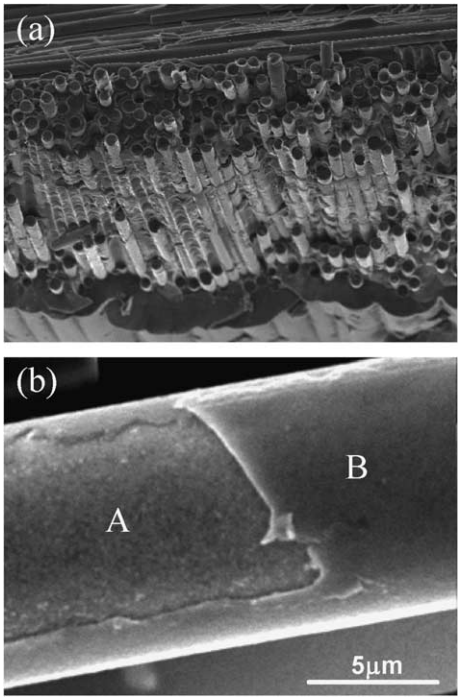

Fig. 1. (a) is the SEM image for fiber push-out tension test. (b) is the high magnification SEM image of pull out fiber.

this Figure, the thickness of PyC interphase layer is about 60–80 nm. The microstructure in fiber is amorphous carbon mixed with SiC grains and column-like structure in matrix. Besides, there are some cracks which were observed between the carbon interphase and fibers at specimen preparation process. This result reveals that the interfacial bonding of some PyC interphase/fiber is weaker than the matrix/PyC interphase. The energy-

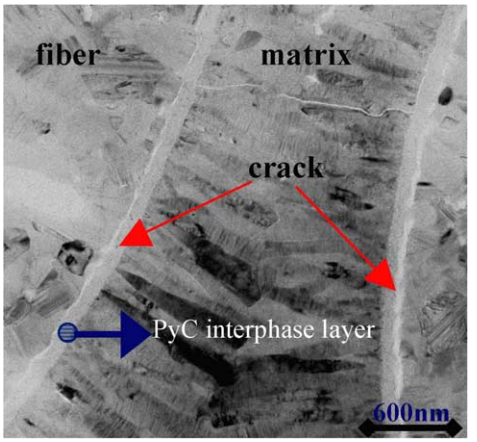

Fig. 2. The cross-section TEM image of Tyranno-SA SiC/SiC composite.

dispersive X-ray spectra (EDX) were acquired from the mark *A* and *B* in Fig. 1(b). The Si/C ratio in the mark *A* is about 0.9 and very closes to 1 because the microstructure of fiber is SiC grains mixed with amorphous carbon. In the mark *B*, the Si/C ratio is about 0.22 due to fiber covered with stripped PyC layer. The high resolution images for the two interfaces, fiber/PyC interphase/matrix, are represented in the Fig. 3(a) and (b). Observing the interfacial behavior of the PyC interphase/fiber, there is a discontinuous graphite-like interlayer and thickness is about 10 nm. On the contrary, the interface of the SiC matrix and PyC interphase is very uniform and smooth graphite-like structure. According to the above analyses, the behavior of crack propagating and branching is very similar to the conclusion of previous studies [8,24] and the non-uniform bonding strength of PyC layer/fiber interface should be the major

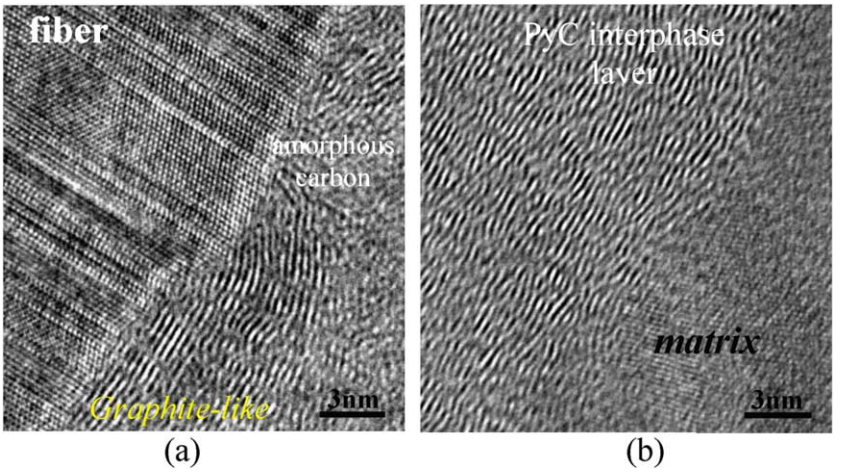

Fig. 3. The high resolution image of (a) PyC interphase/fiber interface. (b) matrix/PyC interphase.

cause of fracture. This is because the non-uniform bonding strength would suppress the ability of fiber sliding which could release external stress or loading.

To verify the above assumption, the advanced ESI technique with carbon core-loss region is used due to its high sensitivity of the π and σ bonding distribution and quantification. The previous study revealed that the morphology of advanced ESI-spectrum is almost similar to the EEL-spectrum [23]. Gaussian distribution is the suitable model for calculating sp^2 and sp^3 bonding content in the EEL-spectra [25]. The completed procedures of advanced ESI and bonding qualification were described and discussed in literature [23,25–28]. After Advanced ESI process and quantification calculation for bonding concentration, the bonding ratio mapping is represented in the Fig. 4. The Fig. 4(a) is the bright field TEM image of SiC/SiC composite and the Fig. 4(b) is the sp^2 fraction mapping of this region. Although high resolution images reveal that both interfaces of fiber/PyC and PyC/matrix exist the graphite-like structure, the sp^2 fraction mapping indicates that the interface of fiber/PyC layer owing higher sp^2 concentration than matrix side and non-uniform distribution. The thickness of high sp^2 bonding layer is about 6–10 nm and consistent with the result of Fig. 3(a). The results reveal the weak bonding strength and non-uniform distribution in the interface between fiber and PyC interphase lead the origin of cracking located at this weak bonding region and propagate till to the strong bonding area. The roughness pull-out fiber surface is caused by the competition of the strong bonding and friction which caused by the roughness of matrix/PyC. Therefore, the sp^2 fraction mapping is strong evidence for supporting our cracking mechanism assumption.

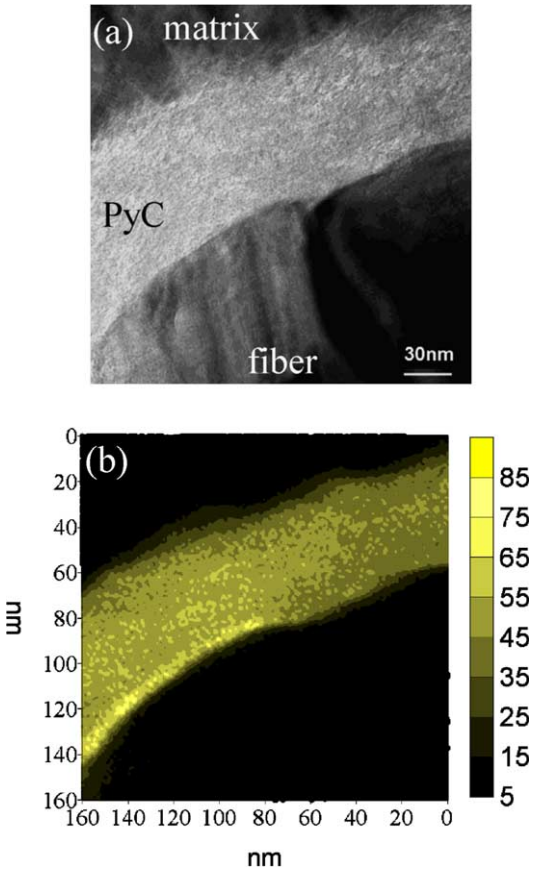

Fig. 4. (a) is the bright field TEM image of SiC/SiC composite and (b) is the sp^2 fraction mapping of PyC interphase layer.

4. Summary

In this article, the characteristic of PyC interphase layer and the cracking mechanism of Tyranno-SA SiC/SiC composites was investigated by the fiber pull-out tension tests, HRTEM and advanced ESI analysis. The advanced ESI mapping technique is excellent tool to study the SiC/SiC composites cracking mechanism. Combining these analyses, the weak bonding and non-uniform distribution of fiber/PyC interphase is the origin of cracking.

Acknowledgements

The Tyranno-SA SiC/SiC composite is supplied by Professor A. Kohyama and Professor Y. Katoh, Institute of Advanced Energy, Kyoto University, Japan. The authors acknowledge form (NSC 90-2212-E-007-028) and (NSC 90-2216-E-007-018).

References

[1] A. Kohyama, M. Seki, K. Abe, T. Muroga, H. Matsui, S. Jitsukawa, S. Matsuda, J. Nucl. Mater. 283–287 (2000) 20.
[2] S.M. Dong, G. Chollon, C. Labrugère, M. Lahaye, A. Guette, J.L. Buruneel, M. Couzi, R. Naslain, D.L. Jiang, J. Mater. Sci. 2371–2381 (2001) 36.
[3] L.L. Snead, R. H Jones, A. Kohyama, P. Fenici, J. Nucl. Mater. 233–237 (1996) 23.
[4] S. Dong, Y. Katoh, A. Kohyama, J. Eur. Ceram. Soc. 23 (2003) 1223.
[5] A. Kohyama, M. Kotani, Y. Katoh, T. Nakayasu, M. Sato, T. Yamamura, K. Okamura, J. Nucl. Mater. 283–287 (2000) 853.
[6] K. Park, T. Vasilos, J. Mater. Sci. 295–300 (1997) 32.
[7] W. Yang, A. Kohayam, T. Noda, Y. Katoh, T. Hinoki, H. Araki, J. Yu, J. Nucl. Mater. 307–311 (2002) 1088.
[8] F. Rebillat, J. Lamon, R. Naslain, E. Lara-Curzio, M.K. Ferber, T.M. Besmann, J. Am. Ceram. Soc. 81 (1998) 2315.

[9] A.J. Frias Robelo, H.W. Scholz, H. Kolbe, G.P. Tartagalia, P. Fenici, J. Nucl. Mater. 258–263 (1998) 1582.
[10] T. Nozawa, T. Hinoki, Y. Katoh, A. Kohayam, J. Nucl. Mater. 307–311 (2002) 1173.
[11] J. Meyer, J.M. Plitzko, J. Microsc. 183 (1996) 2.
[12] P. Kovarik, E.B.D. Bourdon, R.H. Prince, Phys. Rev. B. 48 (1993) 12123.
[13] L. Laffont, M. Monthioux, V. Serin, Carbon. 40 (2002) 767.
[14] H.R. Daniels, R. Brydson, A. Brown, B. Rand, Ultramicroscopy 96 (2003) 547.
[15] D. Pines, Rev. Mod. Phys. 28 (1956) 184.
[16] O.L. Krivanek, M.K. Kundmann, K. Kimoto, J. Microsc. 22 (1995) 180.
[17] K.T. Moore, J.M. Howe, D.C. Elbert, Ultramicroscopy 80 (1999) 203.
[18] C. Jeanguillaume, P. Trebbia, C. Colliex, Ultramicroscopy 3 (1978) 237.
[19] J.M. Martin, B. Vacher, L. Ponsonnet, V Dupuis, Ultramicroscopy 65 (1996) 229.
[20] J. Mayer, U. Eigenhaler, J.M. Plitzko, F. Dettenwanger, Micron 28 (1997) 361.
[21] P.J. Thomas, P.A. Midgley, Ultramicroscopy 88 (2001) 179.
[22] S.C. Lo, J.J. Kai, F.R. Chen, L.C. Chen, L. Chang, C.C. Chiang, P. Ding, B. Chin, H. Zhang, F. Chen, J. Electron. Microsc. 50 (2001) 497.
[23] J.Y. Yan, F.R. Chen, J.J. Kai, J. Electron. Microsc. 51 (2002) 391.
[24] C. Droillard, J. Lamon, J. Am. Ceram. Soc. 79 (1996) 849.
[25] A.J. Papworth, C.J. Kiely, A.P. Burden, S.R.P. Silva, G.A.J. Amaratunga, Phys. Rev. B. 62 (2000) 12628.
[26] S.D. Berger, D.R. McKenzie, Philos. Mag. Lett. 57 (1988) 285.
[27] C.A. Davis, G.A.J. Amaratunga, K.M. Knowles, Phys. Rev. Lett. 80 (1998) 3280.
[28] A.C. Ferrai, B.K. Tanner, V. Stolojan, L.M. Brown, S.E. Rodil, B. Kleinsorge, J. Robertson, Phys. Rev. B. 62 (2000) 11089.